Published in final edited form as:
Neuroscience. 2007 May 25; 146(3): 974–985.

Viral Regulation of the Long Distance Axonal Transport of Herpes Simplex Virus Nucleocapsid

Jennifer H. LaVail[1], **Andrew N. Tauscher**[1], **Anatol Sucher**[1], **Ons Harrabi**[1], and **Renato Brandimarti**[2]

1 *Departments of Anatomy and Ophthalmology, University of California San Francisco, San Francisco, CA94143-0452 USA*

2 *Laboratories of Microbiology and Virology, Department of Experimental Pathology, University of Bologna, Bologna, Italy*

Abstract

Many membranous organelles and protein complexes are normally transported anterograde within axons to the presynaptic terminal, and details of the motors, adaptors and cargoes have received significant attention. Much less is known about the transport in neurons of non-membrane bound particles, such as mRNAs and their associated proteins. We propose that Herpes Simplex virus type 1 (HSV) can be used to study the detailed mechanisms regulating long distance transport of particles in axons. A critical step in the transmission of HSV from one infected neuron to the next is the polarized anterograde axonal transport of viral DNA from the host infected nerve cell body to the axon terminal. Using the *in vivo* mouse retinal ganglion cell model infected with wild type virus or a mutant strain that lacks the protein Us9, we found that Us9 protein was necessary for long distance anterograde axonal transport of viral nucleocapsid (DNA surrounded by capsid proteins), but unnecessary for transport of virus envelope. Thus, we conclude that nucleocapsid can be transported independently down axons via a Us9-dependent mechanism.

Keywords

HSV; capsid; anterograde; neuron; polarity; particle

INTRODUCTION

The highly polarized neuron has discrete functional regions that are maintained in part by the active transport of materials along cytoskeletal filaments and on diverse cytoplasmic motor enzymes. A critical tool in many transport studies has been viral transfection by which viral proteins are targeted preferentially to axons or dendrites [1]. In these experiments, viral particles exploit machinery that establishes and maintains neuronal polarity for selective, directional movement in neurons, and thus, examination of viral transport within neurons gives insight into host cell transport mechanisms.

Herpes simplex virus type 1 (HSV) is commonly found in the general population. HSV infects between 60% and 95% of the adult population world-wide and HSV encephalitis is the most

Corresponding author: Jennifer LaVail, Ph.D., Department of Anatomy, University of California San Francisco, San Francisco, CA 94143-0452, Ph.: 415 476-1694, Fax: 415 514-3933, e-mail: lavailj@vision.ucsf.edu

common cause of sporadic, fatal encephalitis [2–4]. HSV can initially infect the corneal epithelium, oral mucosa or other mucous membranes, then can invade sensory nerve endings in these epithelia and can travel retrograde within sensory axons. Once in the neuron cell body of the sensory neuron, it may replicate and form new virus or establish a latent infection. After reactivation from latent infection, newly synthesized virions are transported by anterograde axonal transport in the peripheral branch of the axon back to the periphery where they can cause secondary infections producing epithelial scarring. Alternatively, if the virus is transported within the central branch of the axon, it can cause viral encephalitis.

To spread to new host cells, the virus must overcome several obstacles. 1) The virus must travel long distances from the periphery to the ganglion cell body; in humans this distance may be as long as a meter. If it were transported by diffusion alone a new virion would require months between initial production to infection of a second host cell. 2) The virus must travel selectively in a retrograde direction at one stage of infection and travel in an anterograde direction in the same axons at a later stage of infection. 3) HSV is among the largest of neurotropic viruses (> 200 nm in diameter) and it must be transported within very small caliber, unmyelinated axons in the nervous system, e.g., < 500 nm in diameter in the optic nerve [5] and as small as 100 nm in sympathetic nerves [6].

To move rapidly within the relatively thin and long sensory axon, HSV presumably uses the transport mechanisms of axons that normally maintain polarity and supply synaptically related proteins to axon terminals. In this paper, we shall consider only the stage of secondary infection after new viral assembly in the neuron soma. Specifically, we shall focus on the anterograde transport of capsid and DNA in the axon. Virion particles that are newly synthesized in the neuron cell body undergo a sequential process of maturation that ultimately results in the production of a variety of morphological forms and subassemblies [7,8].

There is active debate about how new virus is delivered for long distance transport in axons. One possibility is that the complete virion with envelope and nucleocapsid is enclosed in a host cell vesicle [9]. Another possibility is that the virus travels in at least two subassemblies. One subassembly consists of viral envelope proteins and associated proteins in a host cell vesicle. The other subassembly is a relatively small particle, the capsid that encases the viral DNA. The capsid and its movement along the axon are the focus of this study. It has been hypothesized that that this small ~125 nm wide particle can move without surrounding host membrane through the axoplasm (LaVail et al. 2005) (Fig. 1). Host cell motors have been hypothesized to actively transport the nucleocapsids [10]. Lastly, the capsid and DNA presumably have specific tegument proteins that facilitate binding to plus-end directed axonal transport motors and thus target the viral DNA for anterograde axonal transport to the terminals [11]. The identity of specific proteins that are necessary for the polarized, anterograde transport of viral capsid and DNA is unknown.

Using the HSV infected murine retinal ganglion cell model, we have identified a specific protein, Us9, that is needed for anterograde axonal transport of HSV DNA and capsid [12, 13]. Although several investigators have described a function for HSV Us9 protein in transneuronal transport between infected cells, the precise mechanism and role in transport, whether in viral replication, egress or axonal transport or transneuronal transfer, remain unclear [14,15]. Our results demonstrate that Us9 is necessary for the efficient anterograde transport specifically of viral capsid and DNA, but not the transport of viral envelope membrane glycoproteins to axon terminals. Together these results show that virus is transported in the anterograde direction, not as a whole viral particle, but as separate nucleocapsid and viral membrane components via distinct transport mechanisms. Furthermore, the transport of HSV nucleocapsid can be used as a model to study the mechanisms regulating long distance transport of non-membrane bound particles in axons.

EXPERIMENTAL PROCEDURES

Characterization of the *Us9* null and repaired strains

The *Us9* gene in HSV-1 encodes a 90 amino acid protein with a proposed molecular weight of 10,000 [16–18]. The protein has multiple putative post-translational modification sites, e.g., there are 12 serines and 3 tyrosines. Thus, multiple bands are detected in Western blots (Fig. 3B and Fig. 10). An HSV-1 mutant with a single deletion in the *Us9* gene was constructed (Fig. 3A). The BamH1 digestion fragment "X" of the HSV genome was cloned to give pRB124 (1 in Fig. 3A). The pRB124 was digested with BseR1 and then religated to collapse the region between the two BseR1 sites. The resulting plasmid, named pRB5359, contains the first 17 nucleotides of the *Us9* sequence followed by nucleotides 205 through 270 in a different frame (2 in Fig. 3A). PRB5369 was cotransfected with HSV-1 (F strain) genomic DNA into rabbit skin cells. When 100% of the cells were cytopathic, the cells were harvested, centrifuged and the supernatant used to inoculate Vero cells at serial dilutions. After the inoculum was removed, the cells were incubated in a medium containing human IgG to isolate individual plaques. Progeny virus contained in several of the plaques was amplified in Vero cells, and the genomic DNA was extracted from each isolate and analyzed by Southern blot, using pRB124 as probe (Fig. 3B). One isolate was chosen for further characterization and named R6607 (2 in Fig. 3A). For this paper we designate this strain as *Us9-*. To confirm that the deletion did not included more than just the *Us9* gene, we sequenced the *Us8, Us8A* and *Us7* genes and found no alteration in size. Using PCR and primers for *Us9a* (5′ CACGCAATCCCACACAGGAC 3′) and for *Us9* (5′ GAGCAGCCACATCAGGAGC 3′), we confirmed the correct integration of the sequence. The *Us9* deletion was repaired by cotransfection of R6607 genomic DNA with the wild type BamH1 X fragment in pRB124 (3 in Fig. 3). From randomly chosen plaques from this transfection, one isolate containing the wild type BamH1 X fragment was chosen as repaired virus and named R6608. For this paper we designate this repaired strain as *Us9R.*

Preparation of viral stocks

Viral stocks of *Us9-*, *Us9R* and wildtype (wt) (F) strains were grown and maintained as described previously [12]. The virus titer was determined by standard plaque assay [19]. There was no significant decrease in the amount of virus produced by the *Us9-* strain as compared to that produced by the *Us9R* or wt strains.

Antibodies and culture supplies

Monoclonal antibody (gD-1D3) that is specific for HSV-1 glycoprotein D (gD), and rabbit polyclonal antibody (R118) that is specific for gC were provided by Gary Cohen and Roselyn Eisenberg, University of Pennsylvania, Philadelphia, PA. An additional monoclonal antibody specific for HSV-1 gD, (MAB8684) was from Chemicon International, Temecula, CA. The monoclonal antibody, ICP5, is specific for the HSV major capsid protein from Biodesign International (, Saco, ME). Polyclonal rabbit anti-HSV/Horseradish peroxidase (HRP) (#AXL298P) is from Accurate Chemical and Scientific, Westbury, NY. Goat anti-rabbit IgG/HRP (111-035-144) was from Jackson ImmunoResearch Laboratories (West Grove, PA). Goat anti-rabbit IgG/HRP (SC-2004) was from Santa Cruz Biotechnology, Santa Cruz, CA. The ICP5 monoclonal antibody was from Virusys Corporation, Sykesville, MD. It has been successfully used previously at the EM immunocytochemical level to identify capsids that were co-labeled with viral DNA by EM in situ hybridization [13]. We used the "BCA Protein Assay Kit "from Pierce (Rockford, Illinois). A polyclonal rabbit antisera was raised against a peptide containing first 17 amino acids of the *Us9* sequence and was affinity purified by the manufacturer (Zymed, South San Francisco, CA). The bulk of the non-specific immunoglobulin was thus removed. We also obtained pre-immune serum for the same rabbits subsequently used to raise Us9 antibody. All culture supplies were obtained from the Cell Culture Facility, University of California San Francisco.

Intraocular injections

The retinal ganglion cell model several advantages [12,13]. Delivery of virus at the limbus of the eye avoids direct damage to retinal cells. Delivery of antiviral drug 24 hrs postinfection (hpi) restricts the period of viral replication to the first day, effectively providing a pulse infection, and greatly reduces, if not eliminates secondary infection of astrocytes in the optic nerve. The drug also protects the retinal cells from further damage and allows us to study axonal transport in a relatively intact nerve. All procedures involving animals adhered to the Declaration of Helsinki and The Guiding Principles in the Care and Use of Animals and the guidelines of the UCSF Committee on Animal Research. Male BALB/c mice (5–6 weeks of age) were used for all experiments. Eyes were infected with equivalent titers of virus in 4 l of sterile minimal essential medium (MEM) without serum at concentrations of approximately 9×10^4 plaque forming units (pfu), according to a standard procedure [12]. For assays of axonal transport, we introduced Valacyclovir hydrochloride (1 mg/ml) (Valtrex, Glaxo Wellcome, Inc., Greenville, NC) in the drinking water 24 hours after ocular infection [12]. This allow us to "pulse infect" the retinal cells and thus to avoid secondary infection of glial cells in the optic pathway [12].

Tissue isolation for one-step growth kinetics of Us9 mutants

Eyes of mice were infected with viral aliquots as described above. After 6, 12, and 24 hrs the animals were anesthetized and retinas were extracted from the eye [20], placed in 1 ml of PBS (Ca^{++}, Mg^{++} free) with protease inhibitors (Complete Protease Inhibitor Cocktail; Roche Diagnostics GmbH, Mannheim, Germany), homogenized in a dounce homogenizer and frozen at −80 °C. The samples were defrosted, and the homogenate was used to inoculate Vero cells at serial dilutions. The 6 and 12 hr experiments were repeated in quadruplicate, the 24 hr experiments were repeated three separate times in quadruplicate.

Tissue isolation for assay of axonal transport

The eyes of mice were infected with approximately 6×10^5 pfus. After 3 or 5 dpi, the animals were anesthetized and each mouse was perfused intracardially with 20 ml of saline. The optic nerves, extending from the orbit to the optic chiasm, were removed following a standard protocol [12]. The optic chiasm (OC) was dissected from the hypothalamus and the portions of the optic nerve adjacent to the optic chiasm (ON2) and of the optic tracts (OT) were dissected (Fig. 2). The portion of the optic nerve near the retina was not included, because past experiments have demonstrated a leakage of virus in this region that was not directly related to axonal transport [12]. As a negative control, optic tracts of uninfected mice were similarly prepared. The same experiment was repeated 3 to 4 times for each time point. To control for possible vascular transfer of virus, we took samples of cerebellum from infected mice. We failed to find any viral DNA in this control tissue. Aliquots of viral stocks were used as positive controls for viral proteins with no mouse antigens.

PAGE and Western blots

Retinas were dissected 24 hpi from mice infected with equivalent titers of wt, *Us9*- and *Us9R* strains. The protein concentrations of retinal homogenates were determined as described previously (LaVail et al., 2005). Equivalent amounts of protein were loaded on SDS PAGE and transferred and blotted with the Us9 antibody (C in Fig. 3). The optic pathways were dissected and prepared for SDS-PAGE and Western blots with antibodies to VP5, to gD and gC, two of the major viral envelope proteins, and to Us9 protein, according to previously published procedures [12]. When we omitted the primary monoclonal antibody in Western blots and incubated in sheep anti-mouse antisera, we consistently found a band at ~55 kDa in all lanes. This represents the non-specific binding of the secondary antibodies to the heavy chain of the IgG present in mouse samples. When we omitted the second antibody, we saw no

bands on the immunoblots. To control for this non-specific binding, we included tissue samples from uninfected animals in these assays. Samples of viral stocks were run as positive controls.

PCR analysis

Forward and reverse primers targeting the *Us6* (gD) sequence of HSV-1 were used, as described previously [13]. Aliquots of wt and *Us9R* stocks of HSV were used as positive controls. Aliquots of uninfected mouse brain were used for negative controls. The experiments were repeated three times. The ratio of *Us9*- DNA to wt DNA was determined for each experiment using NIH Image J software.

Immunohistochemistry

For light microscopic immunohistochemistry to determine the transport of virus to second-order neurons in the CNS, we inoculated the eyes of mice with each of the three strains of virus (as described above). The mice were allowed to survive for 5 days. No Valacyclovir was supplied. The mice were anesthetized, perfused, and dissected as previously described [12]. The brain was dissected and transverse sections of the brain from the level of the anterior thalamic nuclei to the superior colliculi were cut at a thickness of 60 m on a vibratome. The sections were collected in PBS. Sections were incubated overnight in blocking solution (3% normal goat serum (NGS), 0.1% Triton X-100 in PBS) followed by an overnight incubation in polyclonal antibody to human HSV at a 1:100 dilution. The presence of HSV antigens was determined with diaminobenzidine as the substrate, according to standard methods [8].

For electron microscopic (EM) immunohistochemistry to determine the infection of retinal ganglion cell bodies, we injected virus into the eyes of mice with each of the three strains according to the standard protocol. The mice were allowed to survive for 24 hrs. They were then anesthetized, perfused and the eyes were dissected as previously described [12]. For EM immunohistochemistry of the distribution of Us9 antigen in retinal ganglion cell bodies and astrocytes, tissues were prepared using the polyclonal antibody to Us9 (1:100 in PBS followed by 1:100 anti-rabbit IgG/HRP). As negative controls, infected tissues were prepared according to the same protocol as the experimental tissues, except that the tissues were incubated in preimmune serum from the rabbit used to raise the Us9 antibody or only in secondary antibody, omitting the primary antibody. There was no background immunostaining in either control tissues. As further control to block non-specific staining of the Us9 antibody to HSV gE/gI that acts as an Fc receptor, we incubated the sections first in pre-immune rabbit serum, then in the anti-Us9 antibody followed by the second antibody. Since we observed Us9 immunostaining over capsids and other membrane structures, we conclude that the Us9 antibody is specific for those structures. The tissue sections were photographed.

To quantify the immunolabeling, the proportion of cell cytoplasm occupied by various organelles was measured using a coherent multipurpose test lattice (spacing 15 mm superimposed on the micrographs) over montages of labeled cells (total magnification = 25,000) [21]. The total retinal ganglion cell area sampled was 64.75 m^2 and 71.90 m^2 for astrocytes. The density of immunolabeled organelles was measured in the same micrographs. The number of point overlying specifically immunopositve organelles divided by the total number of point over all of the organelles is the density of labeled organelles. Frequencies of observed and expected densities were compared using a Chi-square test for goodness of fit [22].

Co-immunoassays

The association of the Us9 protein with the capsid was investigated biochemically using immunoaffinity assays. Animals were infected with wt HSV according to the standard protocol. Valacyclovir was provided. At 5 dpi the animals were euthanized and the optic pathways

collected for analysis. The lysate included infected retinal ganglion axons in the optic pathway [12]. We prepared an immunoaffinity matrix with a rabbit polyclonal antibody to Us9 covalently linked to sepharose beads. A lysate of the optic pathways was mixed with the beads. Following washing, the protein was eluted, run on SDS PAGE and transferred to PVDF membrane. The Western blot was probed with the polyclonal anti-Us9 antibody or anti-VP5 antibody. As a control the lysate was also incubated with beads coupled to equivalent amounts of purified rabbit IgG. The experiment was repeated five times. Additional blots of the eluate were prepared and probed with antibodies to gC and gB, and no protein bands were detected (data not shown).

RESULTS

Us9-, *Us9R* and wild type viruses infect the retina

We determined that the Us9 protein is not necessary for normal production of infectious virus in retinal cells. Viral titers in the retinas were assayed at 6, 12, 24 and 48 hpi with 5.5×10^4 pfu of *Us9-*, *Us9R* or wt strains. The titers were expressed as pfu per retina. A significant fraction of all three viral inocula was lost during the first 6 hrs; all were less than 10% of the original inoculum (data not shown). We attribute this loss to the eclipse phase of the infection [23]. By 24 hrs, the concentration had increased to 1.24×10^4 pfu (n = 3), 2.22×10^4 pfu (n = 2) and 3.06×10^4 pfu (n = 2) for wt, *Us9R* and *Us9-*, respectively. The titers of the three viral strains that were recovered 24 hpi from infected mice were ranked and compared statistically with one another, using the Mann-Whitney U test [22]. There was no significant difference between strains at a critical value of $p < 0.01$. Thus, the amounts of infectious virus in the retina are similar for the three strains at 24 hpi, the time when we introduce Valacyclovir in the drinking water. We conclude that Us9 protein is not necessary for production of infective virions in retina.

To confirm that the ganglion cells were infected with all viral strains, we used EM immunohistochemistry with polyclonal antisera to HSV. The retinas were infected with wt, *Us9R* and *Us9-* strains of virus and retinas were collected 24 hpi. We demonstrate that both capsids (asterisk) and enveloped capsids can be found in the proximal portion of wt infected retinal ganglion cell axons (Fig. 4A). We base our identification of capsids on previous work in which we identified capsids by both EM immunohistochemical staining and EM *in situ* DNA hybridization [13]. After infection with the *Us9R* we found similar capsid-like immunostained particles (asterisk) in the cytoplasm of retinal ganglion cells (Fig. 4B, and inset). After infection with *Us9-* we found that the retinal ganglion cell bodies contained multiple vesicular organelles with immunostaining on the cytoplasmic surface. Small capsid-like profiles (asterisk) were also found in the cytoplasm (Fig 4C and inset). Thus, all three viral strains were capable of infecting retinal ganglion cells. These results confirm earlier EM immunohistochemical findings that Us9 protein associates with both enveloped and unenveloped nucleocapsids in the cytoplasm of wt infected dorsal root ganglion cell bodies *in vitro* [24].

Anterograde transport of viral proteins and DNA

Western blots with antibodies to gD and gC (viral envelope glycoproteins) and to VP5 (capsid protein) were prepared using lysates of the axons of retinal ganglion cells infected with *Us9-* or *Us9R* virus (Fig. 5). By 5 dpi we could detect gD and gC as well as VP5 in the optic tract of ganglion cells of the *Us9R* infected mice (Fig. 2, OT; Fig. 5 A lane OT). This is the time that it takes these markers to travel this far in wt infected mice, indicating that the transport of these two envelope proteins and this capsid protein are unimpaired. In contrast, by 5 dpi we could not detect the capsid protein VP5 in the optic tract of the *Us9-* infected mice, although gD and somewhat less gC could be detected (Fig. 5B). These results support the conclusion

that Us9 protein is required for normal capsid transport, but are not required for the normal transport of at least two major envelope proteins.

Previously, we had established that the wt viral capsid and viral DNA are colocalized in organelles in the mouse optic tract following retinal infection [13]. To determine if the anterograde transport of viral DNA was dependent on *Us9* expression, PCR probes to genomic gD DNA were used to detect viral DNA in the optic pathway 3 dpi with the *Us9*- and *Us9R* strains. HSV DNA was detected in infected optic tracts of the *Us9*- and *Us9R* strains (Fig. 6A). No DNA was detected in control tissue from uninfected animals. However, based on densitometric scans of the PCR bands, only about 7% (S.D. = 5.5%, n = 3) of the DNA was transported by the axons infected with *Us9*- strain as compared to that of the *Us9R* strain (Fig. 6B). Thus, loss of the Us9 protein impairs the efficient transport of the viral DNA and transport of VP5 capsid protein.

The anterograde transneuronal transfer of HSV involves the Us9 protein

The anterograde transneuronal transfer of virus, i.e., transfer from the axon terminal of one infected neuron to the cell body of another neuron, is a critical step in the encephalitic spread of virus. To detect the secondary infection, we omitted the Valacyclovir treatment. We found that the wt virus is transported transneuronally in an anterograde direction from retinal ganglion cell body axons to second order neurons in the thalamus by examining the distribution of infected cells in the lateral geniculate nucleus of the mice (Figs. 2 and 7). After intravitreal injection of wt virus, we found that the virally infected glial cells could also be identified in the optic tract as far as the lateral geniculate nucleus. After immunostaining with a polyclonal antibody to human HSV, we found that neurons and glial cells were distributed in clusters within the boundaries of the lateral geniculate nucleus (Fig. 7A). The clusters may be a function of the non-homogeneous infection of retinal ganglion cells in the retina, since each infected ganglion cell send an axon to a limited region of the lateral geniculate nucleus of the thalamus. The distribution of infected cells in the lateral geniculate nucleus of mice infected with *US9R* virus was similar to that seen after infection with wt virus (Fig. 7B). The lateral geniculate nucleus of mice infected with the *Us9*- strain of virus, however, was free of infected cells (Fig. 7C). Only a few infected glial cells in the overlying optic tract contained immunostained label. These results not only confirm the biochemical and PCR results that *Us9* is required for normal anterograde axonal transport, but they also demonstrate that Us9 protein is required for normal transneuronal delivery of infectious virus to neurons in the lateral geniculate nucleus. The failure of the polyclonal antibody to detect viral envelope or other teguments proteins in the nucleus is surprising and will be examined in greater detail in future studies.

In other cells the wt virus can be transported transneuronally in a retrograde direction from infected nerve endings in the iris and ciliary body of the eye to ciliary ganglion (Fig. 2). From the infected neuron cell bodies in this ganglion, the virus can be transferred transsynaptically and be transported retrograde into a second population of neurons located in the Edinger-Westphal nucleus of the midbrain (Figs. 2 and 8). We detected infected neurons in this nucleus following infection with the *Us9*- (Fig. 8) as well as with *Us9R* and wt strains (data not shown). These results confirm our hypothesis that the *Us9*- strain replicates in the eye of the mouse with an efficiency that is indistinguishable from that of the *Us9R* or wt, and that Us9 protein is not required for the retrograde transport of virus.

The association of the viral capsid with the Us9 protein

The involvement of Us9 in the anterograde transport of the viral DNA and capsid VP5 led us to investigate a possible association of Us9 with VP5, which constitutes about 55% of the capsid protein [25]. The Us9 antibody was used to determine the anatomical localization of the protein in retinal ganglion cell bodies of mice 3 dpi with wt virus. The mice were infected

with wt virus, but not treated with Valacylovir, in order to obtain the strongest immunolabeled for each thin section. Using EM immunohistochemistry and the Us9 antibody, we examined the distribution of Us9 antigen in retinal ganglion cells. We expected and found Us9 antigen associated with organelles normally involved in protein synthesis. Thus, the immunolabel was found associated principally with the outer membrane of the nuclear envelope, Golgi complex, and portions of the endoplasmic reticulum. We also found Us9 immunostaining on capsids (arrows) in the cytoplasm of cell bodies (Fig. 9A and B). None of the immunoreactive capsids were enclosed in membrane, although immunonegative capsids could be identified in the same fields (asterisks, Fig. 9B). This variability in immunostaining may be due to properties of the antibody that would recognize epitopes on a subset of capsids, e.g., those that are more mature or destined for axonal delivery.

To quantify the association of capsid and Us9 antibody, we analyzed the distribution of immunoreactive organelles stereologically using a coherent multipurpose test lattice [21]. Only minimal densities of immunoreactive structures (density of 0.02 or less) were detected in the nucleus or over cytoplasm of retinal ganglion cells (Table I). Significantly higher density of labeling was identified over the Golgi complex, endoplasmic reticulum and capsid. This distribution is significantly different from a normal distribution ($X^2 = 22.85$, df = 6, $p < 0.01$; astrocytes, $X^2 = 17.15$, df = 6, $p < 0.01$). Thus, the antibody labels membranous organelles, as well as capsid.

In tissues from the same mice, we found immunostaining of infected astrocytes in the optic path 3 dpi (Fig. 9C). The Us9 antibody labeled organelles, similar those found in neuron cell bodies, i.e., Golgi apparatus, the endoplasmic reticulum and capsids with minimal labeling of the nucleus, cytoplasm, and vesicles (Table II). The distribution was also significantly different than a random labeling pattern ($X^2 = 17.15$, df = 6, $p < 0.01$). \ Based on these results, we conclude that the Us9 protein localizes not only with the membranes of the Golgi apparatus and endoplasmic reticulum, but also with capsids in infected retinal ganglion cells and astrocytes.

In addition, as a further test of the association of the capsid with Us9, we co-immunoassayed lysates of the optic pathways of mice infected with wt virus and treated with Valacyclovir to limit the infection primarily to retinal ganglion cells. We used Sepharose beads conjugated to anti-Us9 antibodies to concentrate the Us9 protein from the lysate. As expected, the fraction eluted from the affinity matrix detected Us9 proteins in a Western blot (Fig. 10A, lane 2). Us9 was also detected in the optic path lysate (Fig. 10A, lane 1). There was no specific immunostaining in uninfected murine brain tissue (Fig. 10, lane 3). After preparing Western blots of the lysate and immunostaining with VP5 antibody we detected VP5 (Fig. 10B, lane 2). The VP5 was not detected in the uninfected murine brain (Fig. 10B, lane 3), although it was clearly detected in the optic path lysate (Fig. 10B, lane 1). When the same blots were stripped or when fresh blots were prepared of the lysate and probed with antibodies to gC and gB, no bands were detected (data not shown).

As a control we repeated the experiments using Sepharose beads coupled to non-specific IgG (Fig. 10, C and D) We were unable to detect Us9 protein in either infected optic pathway or uninfected mouse brain (Fig. 10D, lanes 2 and 3, respectively), after treating the blot with antibody to Us9, although it was detected in the original optic pathway homogenate. We also were unable to detect VP5 in eluate from infected optic pathway or uninfected mouse brain. We did identify VP5 in the orignal homogenate. These results confirm the observations from EM immunohistochemistry that Us9 is associated with capsids. Whether the association is direct or indirect, i.e., mediated through a third party protein that contacts both Us9 and the capsid protein, remains to be determined by other techniques [26].

DISCUSSION

How viral DNA is axonally transported

One important aspect of this study involves a controversy in the field of neurovirology about the identity of the viral particle that carries the DNA in the axonal compartment. The question is relevant to understanding the viral and host transport mechanisms. There are currently two views or models, both of which depend on evidence from tissue culture experiments. In the first, called the single component model, enveloped capsid complete with DNA as well as tegument proteins are transported together within a vesicular organelle and the viral capsid is not exposed to cytoplasm. Ultrastructural and immunohistochemical evidence in support of this single component model has come from studies of embryonic neurons in culture [27–29].

In the second view, two components of the complete virion are transported separately [10, 30]. One component is composed of the capsid (and DNA) in association with specific tegument proteins in the neuronal cytoplasm. The second component is comprised of viral envelope proteins and host membrane that are synthesized and transported independently. Results of immunoelectron microscopy and biochemical reconstitution of capsid motility *in vitro* have supported the two component model [12,28,31,32].

Our results, based on studies of long distance transport in mature axons *in vivo* support the two-component model. Anterograde transport of viral DNA and capsid protein is impaired if Us9 is absent, but the anterograde transport of gC and to a lesser extent gD is not impaired. However, in the most proximal region of the ganglion cell axons in the optic fiber layer, we have identified virions enclosed in vesicular membrane that are similar to those described in the *in vitro* system (Fig. 4A). Thus, enveloped virus in host cell vesicle membrane indeed may be detected near the neuron cell body or sites of exit in axonal enlargements [28,29]. However, such an organelle is not simply transported throughout the length of the mature axon, as proposed by the single component model.

Infected neurons cell bodies contain a mixture of mature and immature viral forms, but some sorting event at the level of the proximal axon apparently limits the displacement of nucleocapsids within the axon. The question arises how the viral components, consisting of a relatively limited variety of types, in the more distal axon are segregated from the multiple forms found in the neuron cell body. An axon-specific mechanism, such as restricted localization of a specific kinesin or kinesin related protein, might limit transport of capsid to the cell body and proximal axon [33–35]. The high density of microtubules in the initial segment and their propensity to bind to particular motor molecules also has been proposed as a potential “fence” to sort motor molecules and secondarily axonally transported elements from the pre-transport population [34]. However, it is unlikely that the initial segment is the precise site of nucleocapsid segregation, since a mixed population of viral structures, including nucleocapsids, can be found immediately beyond the initial segment (Fig. 4A).

The unenveloped capsids that we see in axons *in vivo* are transported naked in the axoplasm, i.e., there is no endosomal or secretory membrane surrounding the capsid. Many membranous organelles and protein complexes are normally transported anterograde within neuronal axons to the presynaptic terminal, and details of the motors, adaptors and cargoes have received significant attention [35,36] In contrast, much less is known about the regulation of transport of non-membrane bound particles in neurons [37]. For example, mRNAs and proteins associated with the mRNA and cytoskeletal polymers require transport motors (presumably kinesin-related) and associated proteins for their delivery to dendrites and axons [38–42]. Identification of the specific motors and associated motor proteins that participate with Us9 in

viral capsid and DNA anterograde transport is extremely important but likely to be a challenging task [43].

Polarized anterograde axonal transport

Although previous studies have demonstrated the role of other proteins in the egress of capsids from the nucleus and transport from nuclear envelope to vesicles in the cytoplasm of cultured cells [44], we have identified a specific protein, Us9, which is necessary for the efficient polarized, anterograde transport of viral capsid and DNA *in vivo*. As found by others, Us9 is not necessary for the polarized retrograde transport of virus [14,45]. We found that the anterograde transport of viral DNA is reduced about 93% when *Us9* is deleted. This persistent 7% could be due to redundant signaling steps; there may be more than one "link protein" and more than one mechanism for directing polarized transport [33,35,46]. Alternatively, the Us9 protein may interact with host or tegument partners that could compensate for the lack of Us9 in the *Us9*- mutant infected mice.

It is important to note that the Us9 protein in Pseudorabies virus (PRV) has also been identified as essential for normal anterograde transneuronal transport [45] and has been characterized as a unique type II tail-anchored membrane protein [47]. Based on its primary sequence and similarity to the homologous protein Us9 of PRV (Brideau, Banfield and Enquist), one would predict that the HSV-1 Us9 is also a type II, integral membrane protein, and it might be expected to localized in the viral membrane. Indeed, our findings support the linkage of HSV Us9; we find immunostaining over the outer nuclear envelope, portions of the Golgi complex and smooth endoplasmic reticulum in neuronal cell bodies. More surprising is the EM immunocytochemical and immunoassay findings of the association of Us9 protein with the viral capsid. This association has not been reported for the PRV Us9 protein. Future studies, including those with purified virions and HSV infected Vero cells, will examine the association of Us9 and capsid in greater detail.

Despite the similarities in the PRV and HSV Us9 proteins, there appear to be functional differences. Contrary to our findings that HSV Us9 is required for normal transport of nucleocapsid and DNA, the PRV protein appears to be necessary for normal transport of the other subassembly, the envelope proteins of the virus, and plays no obvious role in the anterograde transport of nucleocapsids (Tomishima and Enquist, 2001).

Several factors might account for the EM immunocytochemical, biochemical and functional differences of the two mutant strains. The most obvious explanation involves the different experimental systems used to study anterograde transport of PRV and HSV. The PRV results are primarily based on assays using immature neurons without glial investment [48]. Our HSV results are primarily limited to assays of mature neurons and focus on the characteristics of transport within the axon compartment, rather than the whole cell. Clearly, understanding the precise molecular regulation long distance axonal transport of HSV nucleocapsid is likely to be complicated, and will be facilitated by comparisons with other herpesvirus strains and model systems [15,45,49].

In sum, the HSV Us9 protein specifically targets the anterograde axonal transport of capsid protein and DNA to the distal axon. In delivering viral DNA to axon terminals, it supports the transneuronal spread of infectious virus and plays a key role in the neuropathophysiology of herpetic encephalitis. Furthermore, as a model of non-vesicular transport, the anterograde axonal transport of HSV nucleocapsid offers a new biochemical tool for understanding this functional process in normal neurons *in vivo*.

Acknowledgements

This paper is dedicated to the memory of our colleague, James W. Hicks. The work was supported by PHS grants RO1 EY-08773 and EY-13867 as well as by funds from That Man May See, Inc. and Fight for Sight. We thank Drs. G. Cohen and R. Eisenberg for gifts of monoclonal antibodies and Drs. P. Ohara, S. Sidu, D. Cortez and M. Matthes for advice and assistance.

References

1. Jareb M, Banker G. The polarized sorting of membrane proteins expressed in cultured hippocampal neurons using viral vectors. Neuron 1998;20:855–67. [PubMed: 9620691]
2. Cunningham, AL.; Mindel, A.; Dwyer, DE. Sexually Transmitted Diseases. Academic Press; San Diego: 2000. Global epidemiology of sexually transmitted diseases; p. 3-42.
3. Roizman, B.; Knipe, DM. Herpes simplex viruses and their replication. In: Knipe, DM.; Howley, PM., editors. Fields Virology. Lippincott Williams & Wilkins; Philadelphia, PA: 2001. p. 2399-459.
4. Whitley RJ. Herpes simplex encephalitis: Adolescents and adults. Antiviral Res. 2006in press
5. Reese BE. The distribution of axons according to diameter in the optic nerve and optic tract of the rat. Neurosci 1987;22(3):1015–24.
6. Emery DG, Foreman RD, Coggeshall RE. Fiber analysis of the feline inferior cardiac sympathetic nerve. J Comp Neurol 1976;166(4):457–68. [PubMed: 1270617]
7. Mettenleiter TC. Budding events in herpesvirus morphogenesis. Virus Res 2004;106(2):167–80. [PubMed: 15567495]
8. Ohara PT, Chin MS, LaVail JH. The spread of Herpes simplex virus type 1 from trigeminal neurons to murine cornea: an immunoelectron microscopy study. J Virol 2000;74(10):4776–86. [PubMed: 10775616]
9. Card JP, Rinaman L, Lynn RB, Lee BH, Meade RP, Miselis RR, Enquist LW. Pseudorabies virus infection of the rat central nervous system: Ultrastructural characterization of viral replication, transport, and pathogenesis. J Neurosci 1993;13(6):2515–39. [PubMed: 8388923]
10. Diefenbach RJ, Miranda-Saksena M, Diefenbach E, Holland DH, Boadle RA, Armati PJ, Cunningham AL. Herpes simplex virus tegument protein US11 interacts with conventional kinesin heavy chain. J Virol 2002;76(7):3282–91. [PubMed: 11884553]
11. Wolfstein A, Nagel CH, Radtke K, Döhner K, Allan VJ, Sodeik B. The inner tegument promotes herpes simplex virus capsid motility along microtubules in vitro. Traffic 2006;7:227–37. [PubMed: 16420530]
12. LaVail JH, Tauscher AN, Aghaian E, Harrabi O, Sidhu SS. Axonal transport and sorting of herpes simplex virus components in mature mouse visual system. J Virol 2003;77(11):6117–27. [PubMed: 12743269]
13. LaVail JH, Tauscher AN, Hicks JW, Harrabi O, Melroe GT, Knipe DM. Genetic and molecular in vivo analysis of herpes simplex virus assembly in murine visual system neurons. J Virol 2005;79 (17):11142–50. [PubMed: 16103165]
14. Polcicova K, Biswas PS, Banerjee K, Wisner TW, Rouse BT, Johnson DC. Herpes keratitis in the absence of anterograde transport of virus from sensory ganglia to the cornea. PNAS USA 2005;102 (32):11462–67. [PubMed: 16055558]
15. Chowdhury SI, Mahmood S, Simon J, Al-Mubarak A, Zhou Y. The Us9 gene of bovine herpesvirus 1 (BHV-1) effectively complements a Us9-null strain of BHV-5 for anterograde transport, neurovirulence, and neuroinvasiveness in a rabbit model. J Virol 2006;80(9):4396–405. [PubMed: 16611899]
16. McGeoch DJ, Dolan A, Donald S, Rixon FJ. Sequence determination and genetic content of the short unique region in the genome of herpes simplex virus type 1. J Mol Biol 1985;181:1–13. [PubMed: 2984429]
17. Frame MC, McGeoch DJ, Rixon FJ, Orr AC, Marsden HS. The 10K virion phosphoprotein encoded by gene US9 from herpes simplex virus type 1. Virology 1986;150:321–32. [PubMed: 3008413]
18. Brandimarti R, Roizman B. U_S9, a stable lysine-less herpes simplex virus 1 protein, is ubiquinated before packaging into virions and associates with proteosomes. PNAS (USA) 1997;94(25):13973–78. [PubMed: 9391137]

19. Burleson, FG.; Chambers, T.; Wiedbrauk, DL. Virology: A Laboratory Manual. San Diego: Academic Press, Inc; 1992. p. 250
20. Winkler BS. The electroretinogram of the isolated rat retina. Vision Res 1972;12:1183–98. [PubMed: 5043568]
21. Weibel EG, Kistler G, Scherle W. Practical stereological methods for morphometric cytology. J Cell Biol 1966;30:23–38. [PubMed: 5338131]
22. Bancroft, H. Introduction to Biostatistics. New York, New York: Hoeber Medical Division, Harper and Row; 1965. p. 210
23. Döhner K, Radtke K, Schmidt S, Sodeik B. Eclipse phase of herpes simplex virus type 1 infection: Efficient dynein-mediated capsid transport without the small capsid protein VP26. J Virol 2006;80 (16):8211–24. [PubMed: 16873277]
24. Miranda-Saksena M, Armati P, Boadle RA, Holland DJ, Cunningham AL. Anterograde transport of herpes simplex virus type 1 in cultured, dissociated human and rat dorsal root ganglion neurons. J Virol 2000;74(4):1827–39. [PubMed: 10644356]
25. Steven, AC.; Spear, PG. Herpesvirus capsid assembly and envelopment. In: Chiu, W.; Burnett, RM.; Garcea, RL., editors. Structural Biology of Viruses. Oxford University Press; New York: 1997. p. 312-51.
26. Phizicky E, Fields S. Protein-protein interactions: methods for detection and analysis. Microbiol Rev 1995;59(1):94–123. [PubMed: 7708014]
27. del Rio T, Ch'ng TH, Flood EA, Gross SP, Enquist LW. Heterogeneity of a fluorescent tegument component in single Pseudorabies virus virions and enveloped axonal assemblies. J Virol 2005;79 (7):3903–19. [PubMed: 15767393]
28. Saksena MM, Wakisak H, Tijono B, Boadle RA, Rixon F, Takahashi H, Cunningham AL. Herpes simplex virus type 1 accumulation, envelopment, and exit in growth cones and varicosities in mid-distal regions of axons. J Virol 2006;80(7):3592–606. [PubMed: 16537627]
29. Ch'ng TH, Enquist LW. Neuron-to-cell spread of pseudorabies virus in a compartmented neuronal culture system. J Virol 2005;79(17):10875–89. [PubMed: 16103140]
30. Penfold MET, Armati P, Cunningham AL. Axonal transport of herpes simplex virions to epidermal cells: Evidence for a specialized mode of virus transport and assembly. Proc Natl Acad Sci USA 1994 July;91:6529–33. [PubMed: 7517552]
31. Lee GE, Murray JW, Wolkoff AW, Wilson DW. Reconstitution of Herpes simplex virus microtubule-dependent trafficking in vitro. J Virol 2006;80(9):4264–75. [PubMed: 16611885]
32. Snyder A, Wisner TW, Johnson DC. Herpes simplex virus capsids are transported in neuronal axons without an envelope containing the viral glycoproteins. J Virol. 2006 Sept. 26;
33. Klopfenstein D, Vale RD, Rogers SL. Motor protein receptors: moonlighting on other jobs. Cell 2000;103:537–40. [PubMed: 11106727]
34. Nakata T, Hirokawa N. Microtubules provide directional cues for polarized axonal transport through interactions with kinesin motor head. J Cell Biol 2003;162:1045–55. [PubMed: 12975348]
35. Hirokawa N, Takemura R. Molecular motors and mechanisms of directional transport in neurons. Nature Reviews Neuroscience 2005;6:201–14.
36. Goldstein LSB, Yang Z. Microtubule-based transport systems in neurons: the roles of kinesins and dyneins. Ann Rev Neurosci 2000;23:39–71. [PubMed: 10845058]
37. Brown A. Axonal transport of membranous and nonmembranous cargoes: a unified perspective. J Cell Biol 2003;160(6):817–21. [PubMed: 12642609]
38. Bassell GJ, Zhang H, Byrd AL, Femino AM, Singer RH, Taneja KL, Lifshitz LM, Herman IM, Kosik KS. Sorting of b-actin mRNA and protein to neurites and growth cones in culture. J Neurosci 1998;18 (1):251–65. [PubMed: 9412505]
39. Hirokawa N. mRNA transport in dendrites: RNA granules, motors and tracks. J Neurosci 2006;26 (27):7139–42. [PubMed: 16822968]
40. Yan Y, Brown A. Neurofilament polymer transport in axons. J Neurosci 2005;25(30):7014–21. [PubMed: 16049177]
41. Wang L, Brown A. Rapid movement of microtubules in axons. Curr Biol 2002;12:1496–501. [PubMed: 12225664]

42. Galbraith JA, Gallant PE. Axonal transport of tubulin and actin. J Neurocytol 2000;29(11–12):889–911. [PubMed: 11466477]

43. Baas PW, Qiang L. Neuronal microtubules: when the MAP is the roadblock. Trends in Cell Biol 2005;15(4):184–87.

44. Luxton GW, Haverlock S, Coller KE, Antione SE, Pincetic A, Smith GA. Targeting of herpesvirus capsid transport in axons is coupled to association with specific sets of tegument proteins. Proc Natl Acad Sci USA 2005;102(16):5832–37. [PubMed: 15795370]

45. Brideau AD, Card JP, Enquist LW. Role of pseudorabies virus Us9, a type II membrane protein, in infection of tissue culture cells and the rat nervous system. J Virol 2000;74(2):834–45. [PubMed: 10623746]

46. Döhner, K.; Sodeik, B. The role of the cytoskeleton during viral infection. In: Marsh, M., editor. Membrane Trafficking in Viral Replication. Springer; Berlin: 2004. p. 67-108.

47. Brideau AD, Banfield BW, Enquist LW. The Us9 gene product of pseudorabies virus, an alphaherpesvirus, is a phosphorylated, tail-anchored type II membrane protein. J Virol 1998;72(6):4560–70. [PubMed: 9573219]

48. Tomishima MJ, Enquist LW. A conserved a-herpesvirus protein necessary for axonal localization of viral membrane proteins. J Cell Biol 2001;154(4):741–52. [PubMed: 11502759]

49. Cohen JI, Sato H, Srinivas S, Ledstrom K. Varicella-zoster virus (VZV) ORF65 viron protein is dispensable for replication in cell culture and is phosphorylated by casein kinase II, but not by the VZV protein kinases. Virol 2001;280(1):62–71.

Abbreviations

HSV
: herpes simplex virus type 1

PRV
: pseudorabies virus

Us9-
: *Us9*-null

Us9R
: *Us9*-repaired

wt
: wildtype

hpi
: hours post-infection

dpi
: days post-infection

MEM
: minimal essential medium

NGS
: normal goat serum

phosphate buffered saline
: PBS

plaque forming unit
: pfu

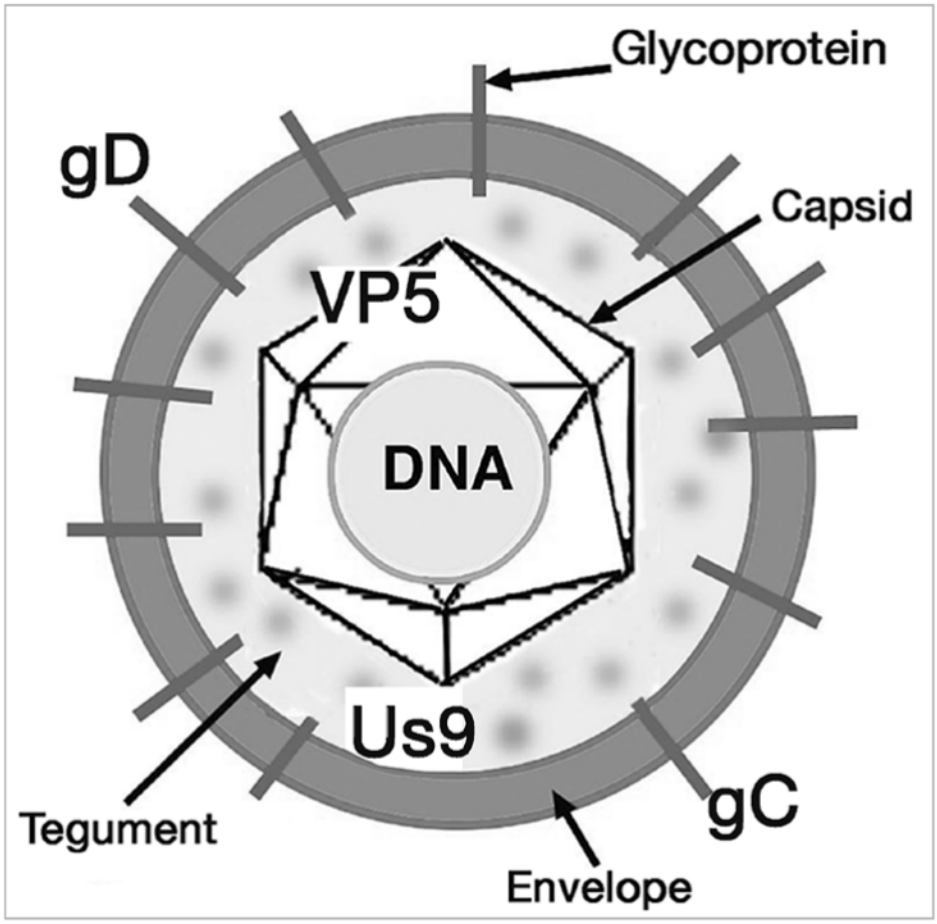

Figure 1.
The structural components of HSV. The infectious form of the virus is composed of a core of DNA surrounded by a protein shell or capsid. The major protein of the capsid is viral protein 5 (VP5). The capsid and DNA, called the nucleocapsid, are surrounded by the glycoprotein-rich envelope composed of eleven proteins. Two of the envelope proteins are glycoprotein D (gD) and gC. The Us9 protein is considered a membrane protein. Between the capsid and the envelope is the tegument, composed of at least 17 proteins.

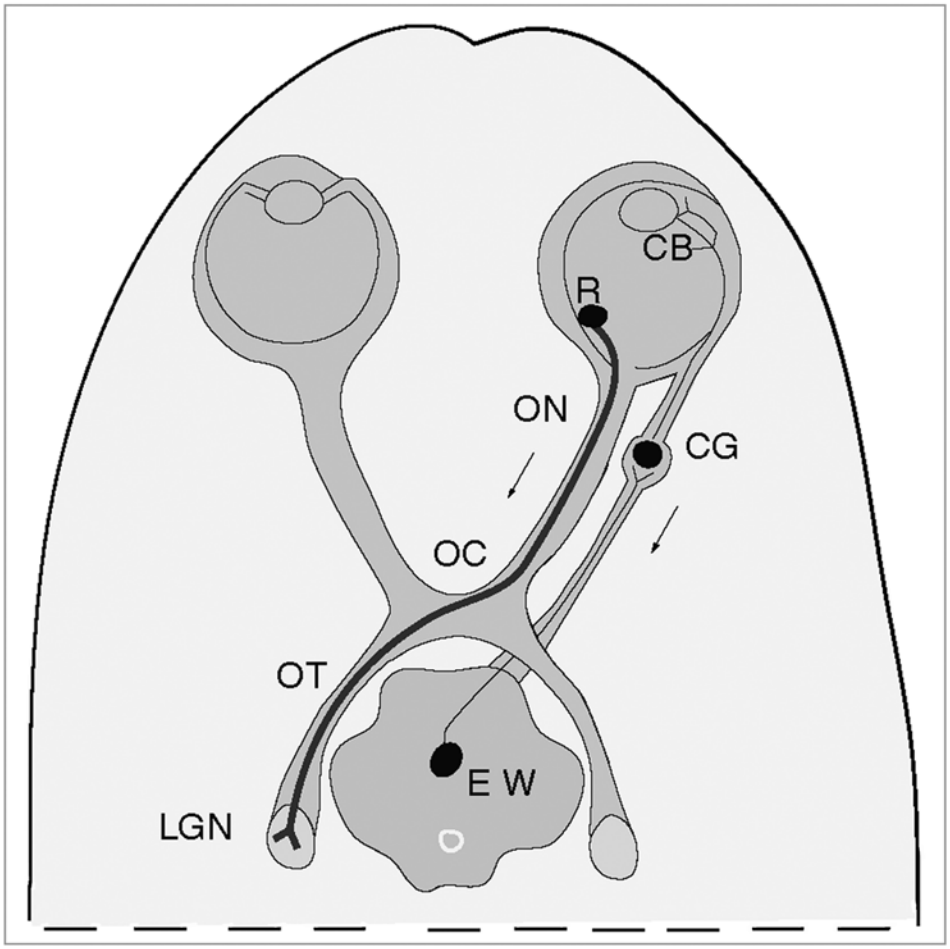

Figure 2.
Diagram of the mouse model of infection. By injecting HSV into the vitreal chamber of the eye, we can infect retinal ganglion cell bodies (R). The anterograde transport of virus can be assayed from retinal ganglion cell bodies, along the axons of the cells in the optic nerve (ON), optic chiasm (OC) and optic tract (OT) to the site of termination in the lateral geniculate nucleus (LGN) of the thalamus. As a result of the same injection we can assay the retrograde transport of virus by axons of ciliary ganglion neurons (CG). From the ciliary body in the eye (CB) the virus is transported retrograde by axons of ciliary ganglion neurons (CG) and then transynaptically to the axons of the neurons of the Edinger-Westphal nucleus (EW) in the midbrain.

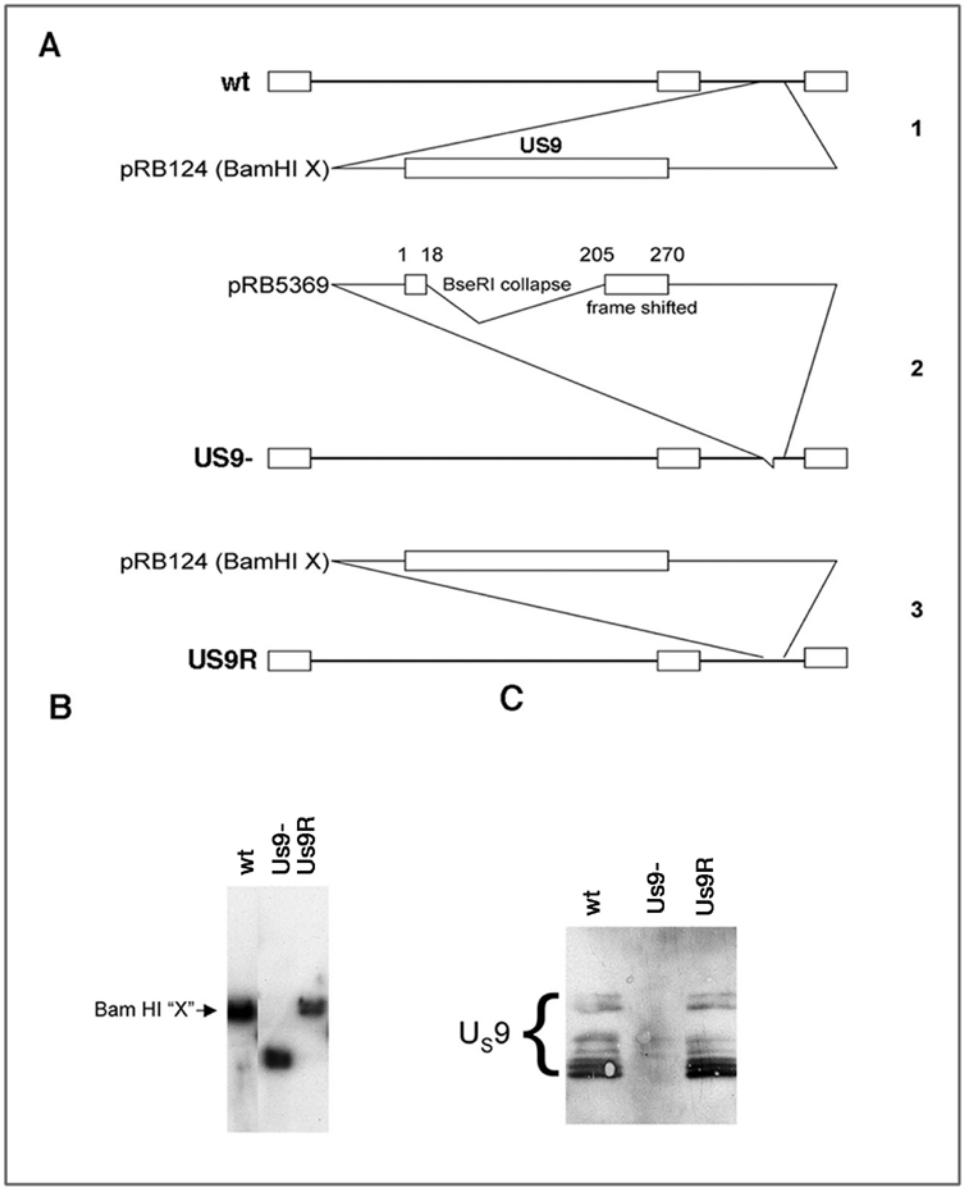

Figure 3.

A. Construction of *Us9* mutant viral stains. 1. Cartoon of genome of F strain virus. *Us9* is located in the unique short regions. The Bam HI digestion fragment (Bam HI X) was used to produce pRB124. 2. The pRB124 was digested with BseR1 and religated to collapse the region between the two BseRI sites. PRB 5369 was generated. This contained the first 18 nucleotides of the US9 sequence and nucleotides 205–270 were frame shifted. pRB 5369 was used to isolate the mutated virus called US9-. 3. The rescued version was generated by co-infection of cells with *US9*- DNA and the wt fragment in pRB124. The selected isolate was named *Us9R*. B. Southern blots of DNA from the viral stocks. The size of fragments from the wt and *Us9R* are indistinguishable. The *Us9*- fragment is smaller than the other two strains. C. Western blots of Us9 protein expressed in retinas by the three strains. The immunobands indicating the presence of the several forms of Us9 protein (bracket) are indistinguishable in retinas infected with the wt and *Us9R*. The Us9 proteins were not expressed in the retinas infected with the *Us9*- strain.

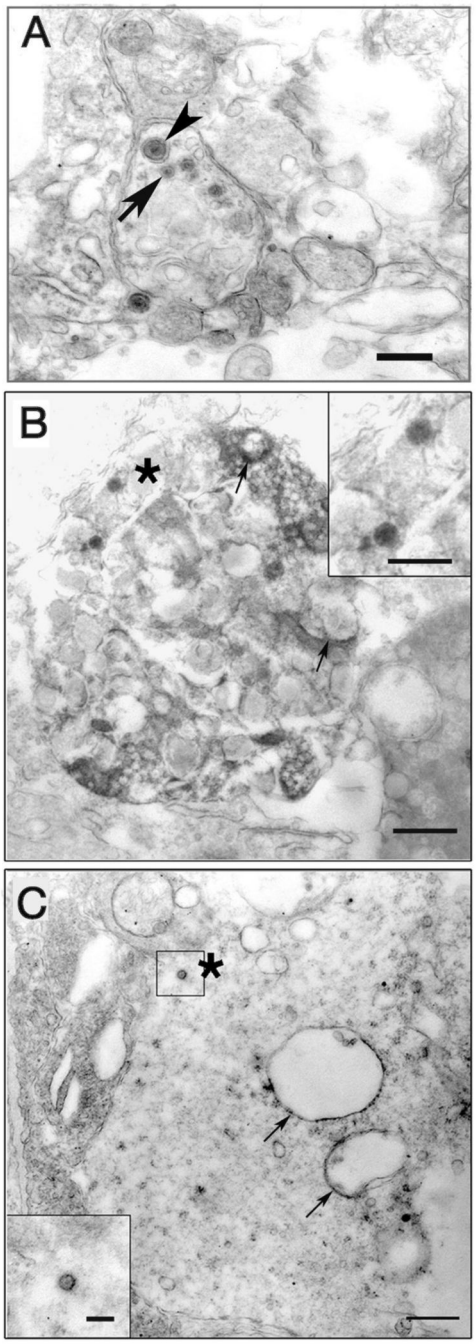

Figure 4.

EM immunohistochemistry of virally infected retinal ganglion cells 24 hr pi. A. Infection with wt strain. Retinal ganglion cell axons are concentrated in a zone immediately adjacent to retinal ganglion cell bodies. Both enveloped (arrowhead) and unenveloped capsids (arrow) can be seen in the axon. Bar = 0.5 m. B. Retinal ganglion cell infected with *Us9R* virus. Viral antigen is concentrated on the surfaces of larger vesicles (arrows) as well as on capsids (asterisk) in the cytoplasm. Bar = 0.5 m Inset, enlarged capsid. Bar = 200 nm. C. *Us9*- infected ganglion cell body with immunostained vesicles (arrows) and a capsid (asterisk) in the cytoplasm. Bar = 0.5 m, inset Bar = 200 nm.

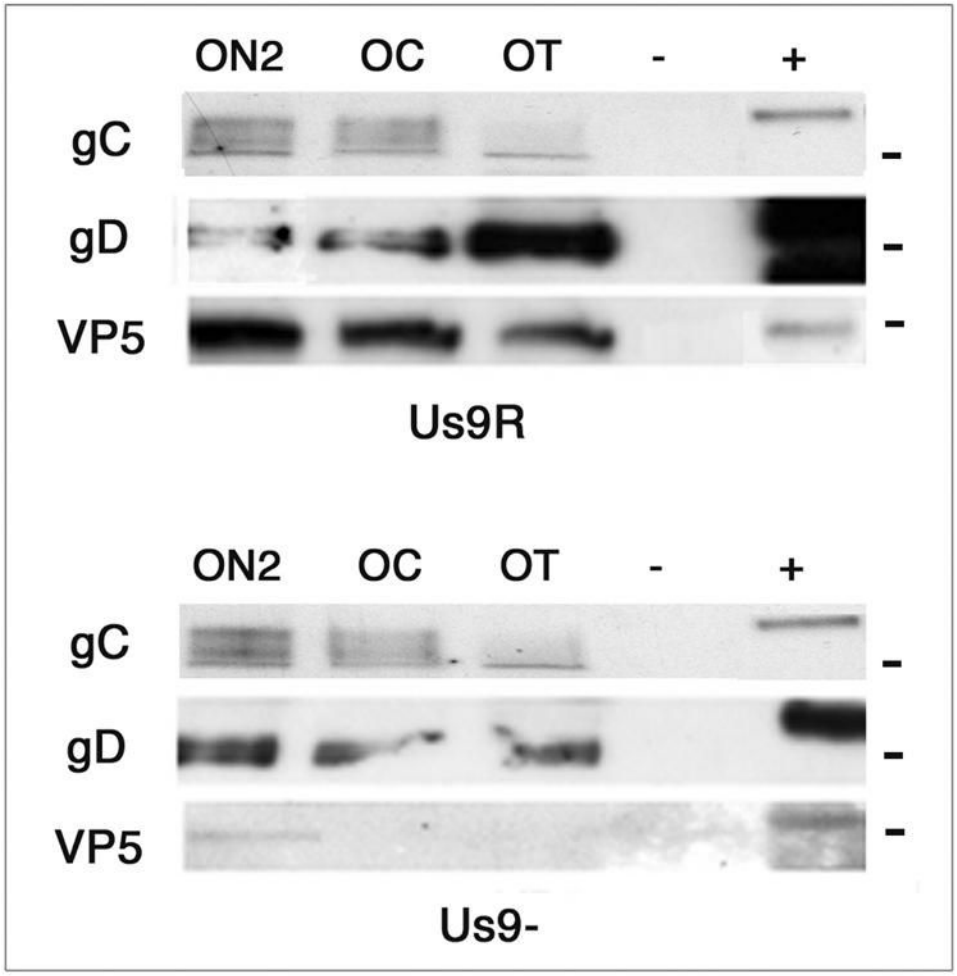

Figure 5.

A. B. Western blots of gC, gD and VP5 proteins in optic pathway of animals infected with *Us9-* and *Us9R* viruses 5 days pi. ON2, optic nerve; OC, optic chiasm; OT, optic tract; - uninfected animal; +, viral stock. A. By 5 days the gC, gD and VP5 proteins are detected throughout the pathway in the *Us9R* infected animals. B. By five days the gC and gD proteins are detected throughout the pathway, but the VP5 capsid protein was detected only in the ON2 of *Us9R* infected mice. −, uninfected tissue; +, viral stock aliquot. The molecular markers are 110, 58 and 155 kDa, from top to bottom.

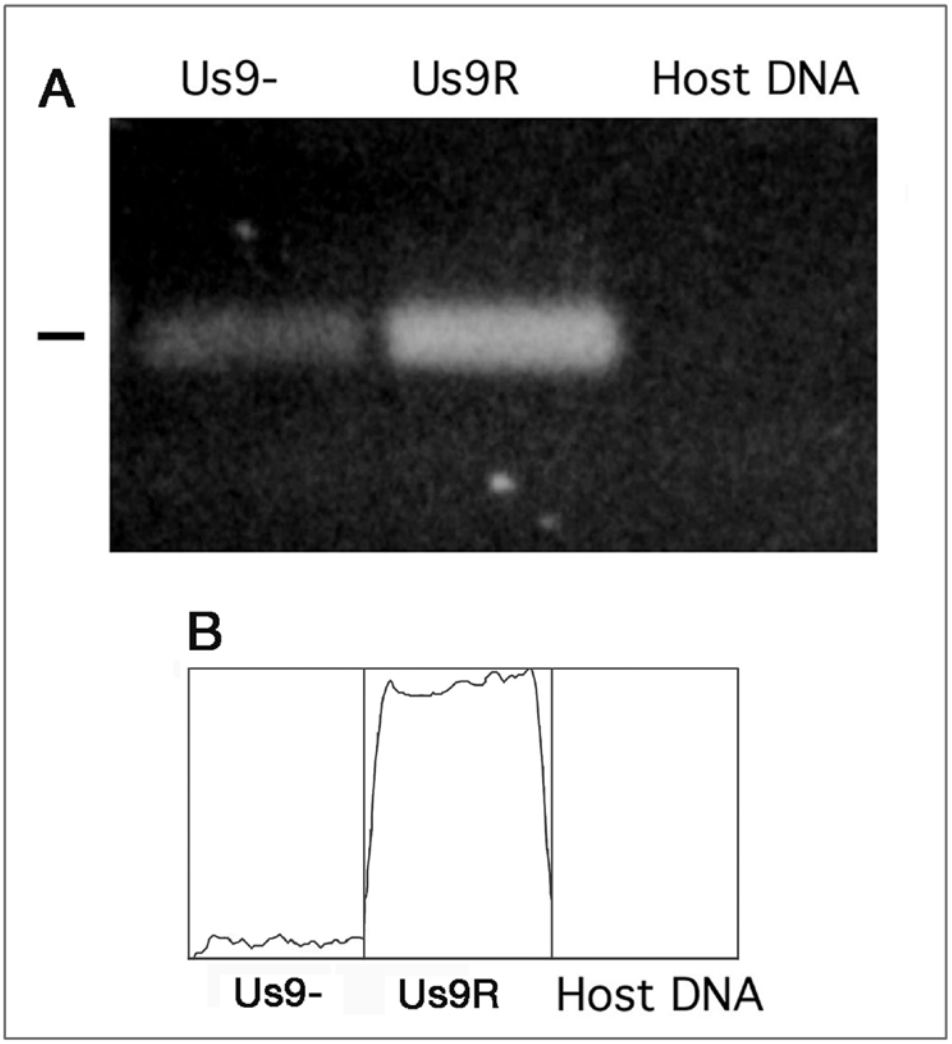

Figure 6.

A. Viral DNA was detected in the optic tract at 3 days pi. The mutant (*Us9*-) and repaired (*Us9R*) both are transported in the axons; the amount of DNA is quantitatively less in the mutant, however. No viral DNA was detected in uninfected mouse brain. B. Densitometry scan of the viral DNA in the *Us9*-, *Us9R* and uninfected host DNA control lanes. The *Us9*- had 7% of the DNA detected in the *Us9R* lane.

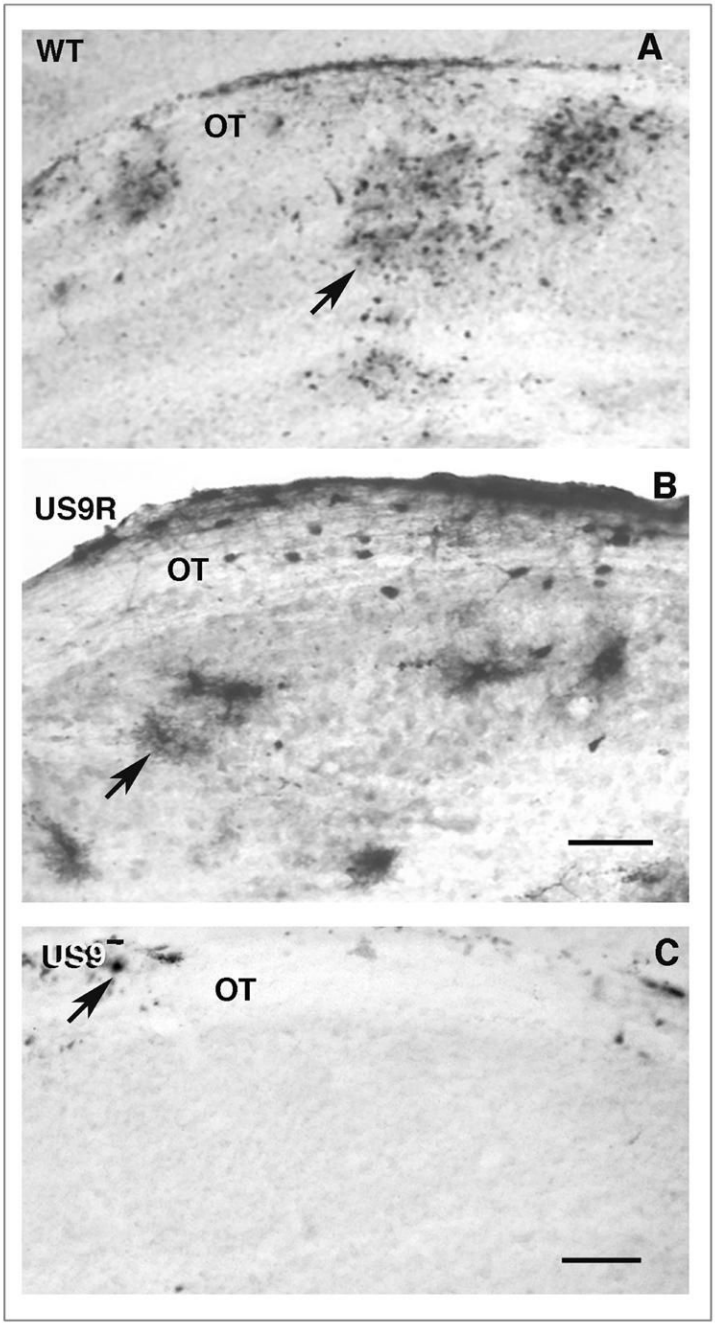

Figure 7.

Anterograde transneuronal transport of viral strains. A polyclonal antisera directed against human HSV was used to detect antigens in the lateral geniculate nucleus 5 days after infection with wt (A), *Us9R* (B) or *Us9*- (C) strains. A and B. The wt and *Us9R* infected nucleus contain clusters of infected neurons and glial cells (arrows). The *Us9*- infected nucleus contains no immunoreactive cells, although there are a few positive glial cells (arrow) in the adjacent optic tract. A and C, bar = 150 um. B, bar = 175 m.

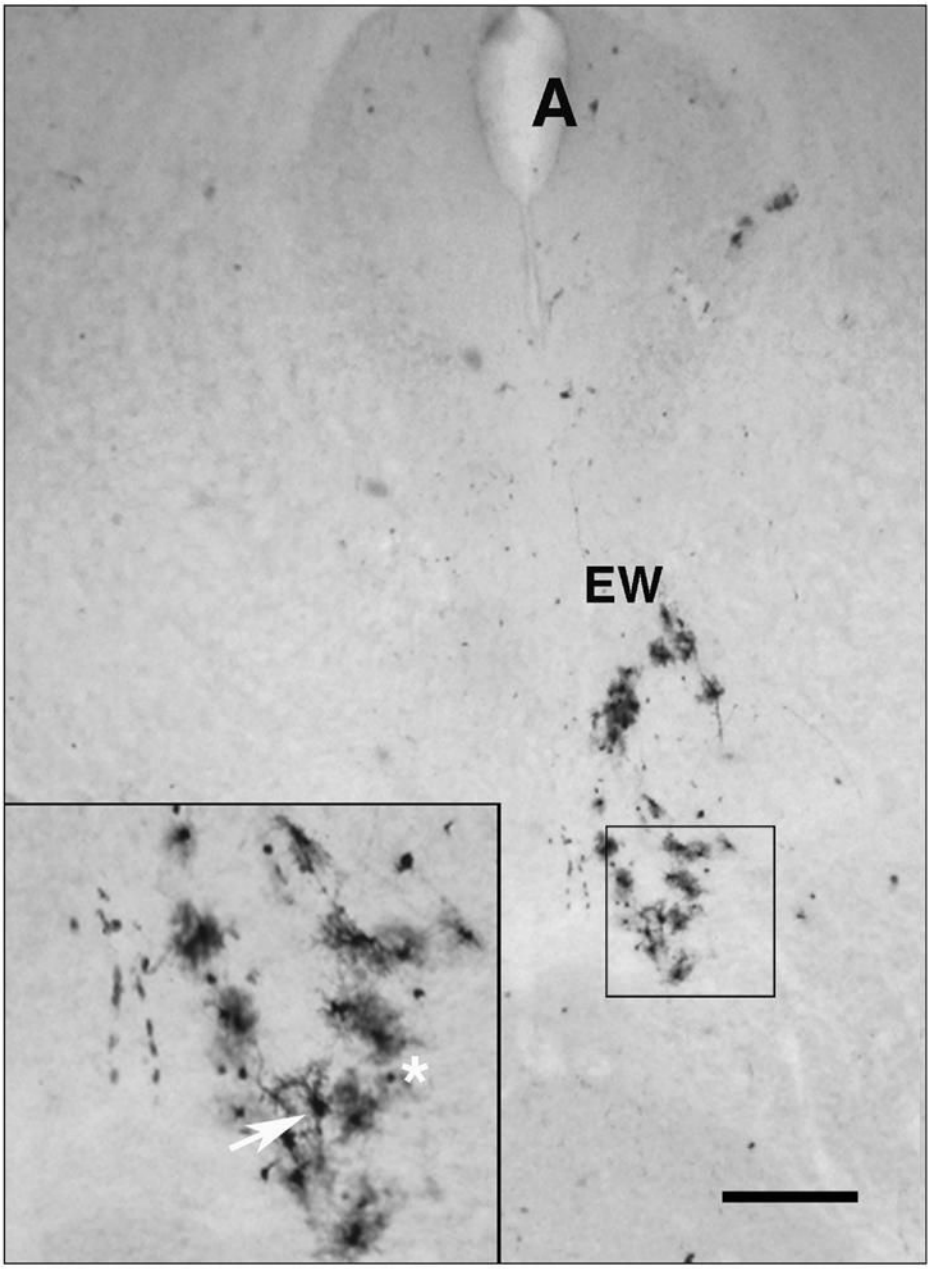

Figure 8.

The *Us9*- strain is transported transynaptically in the retrograde direction in parasympathetic neurons. Neurons in the Edinger-Westphal (EW) division of the oculomotor nerve nucleus are infected. Inset, enlarged view of infected neurons (arrow) and glial cells (asterisk). A, Aqueduct of Sylvius. Bar = 350 m.

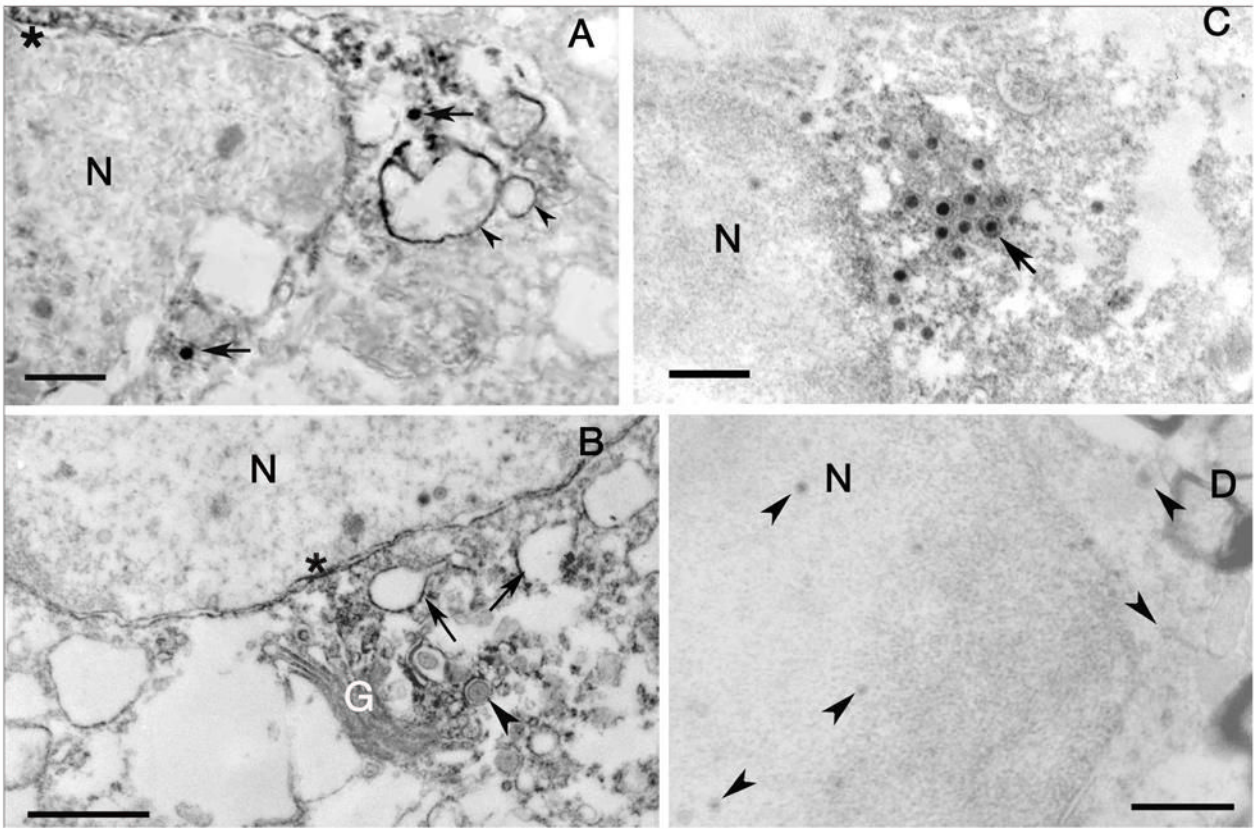

Figure 9.

A. EM immunohistochemistry of Us9 labeling of retinal ganglion cell bodies. The capsids (arrows) in the cytoplasm are immunopositive. The label is also seen over vesicles (arrowheads) and portions of the outer nuclear envelope membrane (asterisk). Bar = 550 nm. B. Portions of the Golgi complex (G) are immunoreactive, as are vesicles (arrows) in the cytoplasm and portions of the nuclear envelope (asterisk). Note that the capsid surrounded by membrane is not immunoreactive (arrowhead). Bar = 1.0 m. C. EM immunohistochemistry of Us9 labeling of an astrocyte in the optic nerve. Both enveloped and unenveloped immunoreactive capsids (arrow) are concentrated near and within other vesicular structures. The nuclear envelope is also immunolabeled (asterisk). Bar = 550 nm. D. Substituting preimmune serum for the Us9 antibody demonstrates the absence of immunoreactivity and unlabeled capsids (arrowheads). N, nucleus. Bars = 1.0 m.

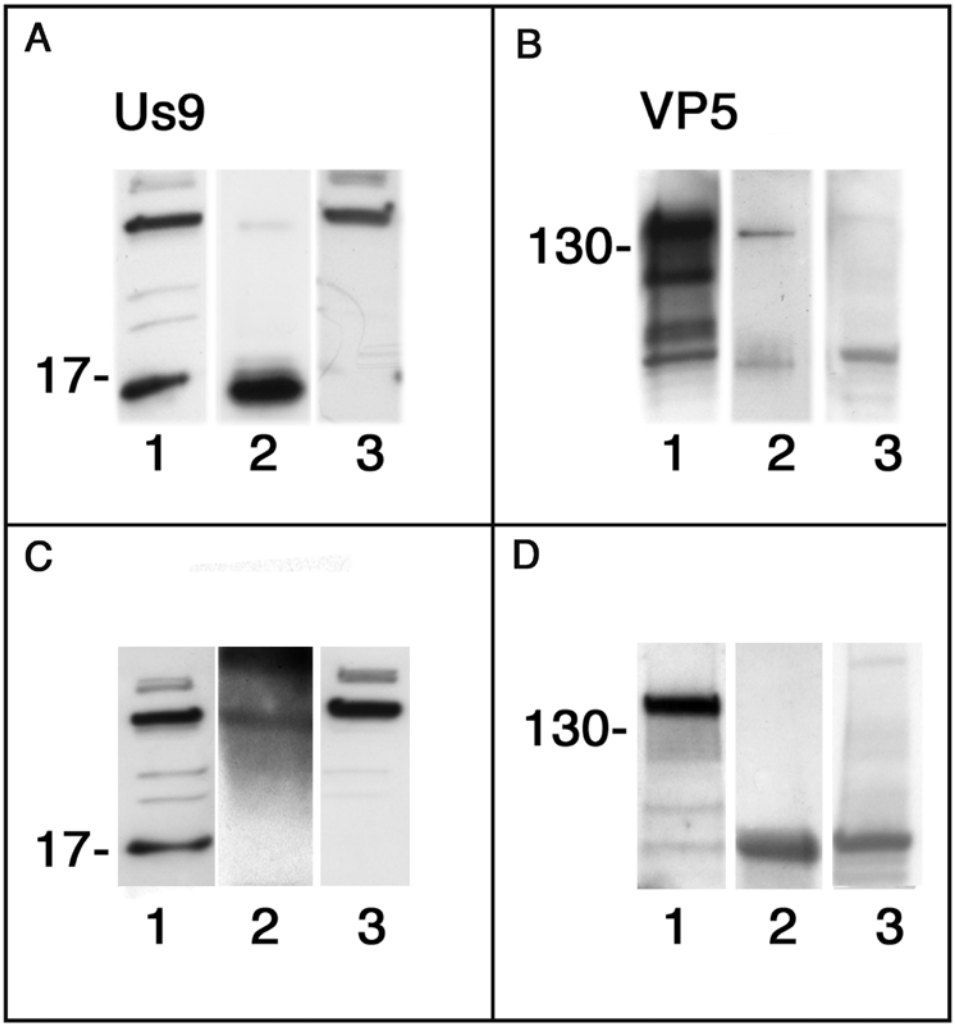

Figure 10.

Comparison of co-immunoassays of lysates of optic pathways of mice infected with wt virus and collected 3 dpi. In each panel lane 1 is a Western blot of lysate before incubation with the beads (positive control), lane 2 is the blot of the elutate fraction and lane 3 is a blot of the eluate fraction from uninfected mouse brain (negative control). A, lane 2 and B, lane 2. We detected both Us9 and VP5 in the lysate affinity assayed with us9 antibody coupled beads. C, lane 2 and D, lane 2. No significant Us9 or VP5 was detected in the lysate affinity assayed with non-specific IgG coupled beads. The molecular weight markers at ~17 kDa indicate one of the multiple forms of Us9. B and D, marker at ~130 kDa.

Table I

Density of Us9-immunopositive elements in retinal ganglion cell bodies of wt infected mice*

Retinal Ganglion cells			
Compartment	**No. of immuno-positive points (% of total)**	**Total points % of total**	**Point density (points/m^2)**
Nucleus	6 (9.2)	260 (16)	0.02
Cytoplasm	7 (10.7)	589 (35)	0.01
Vesicles^	27 (41.5)	152 (9.2)	0.18
Endo. Reticulum	17 (26.1)	22 (1.3)	0.77
Golgi	3 (4.6)	6 (0.01)	0.50
Capsid	4 (6.2)	6 (0.01)	0.66
Unknown	1 (1.5)	34 (2.07)	0.02

* Total area examined was 1068 lattice points and 64.75 m^2.

^ Vesicle category includes vesicles and multivesicular bodies.

Table II

Density of Us9-immunopositive elements in astrocytes in the optic pathway of Us9 wt infected mice*

Astrocytes Compartment	No. immuno-positive points (% of total)	Total points % of total	Point density (points/m^2)
Nucleus	0 (0)	222 (18.8)	0.01
Cytoplasm	1(3.3)	708 (58.5)	0.01
Vesicles^	3 (10)	115 (9.7)	0.12
Endo. Reticulum	7 (23.3)	47 (3.9)	0.77
Golgi	2 (6.6)	24 (0.3)	0.50
Capsid	14 (46.6)	31 (2.6)	0.80
Unknown	3 (10)	36 (2.9)	0.08

*Total area examined was 1186 lattice points and 71.90 sm^2.

^Vesicle category includes vesicles and multivesicular bodies.